Full Paper

Applied Organometallic Chemistry

Received: 27 May 2014 Revised: 30 October 2014 Accepted: 30 October 2014 Published online in Wiley Online Library

(wileyonlinelibrary.com) DOI 10.1002/aoc.3256

Benzimidazole-based silver(I)–*N*-heterocyclic carbene complexes as anti-bacterials: synthesis, crystal structures and nucleic acids interaction studies

Patrick O. Asekunowo[a], Rosenani A. Haque[a]*, Mohd. R. Razali[a] and Srinivasa Budagumpi[b]

A series of new benzimidazolium salts as *N*-heterocyclic carbene (NHC) precursors has been synthesized. Reactions of these salts with Ag_2O with varying metal-to-salt ratio facilitate the formation of a series of new binuclear and mononuclear Ag(I)–NHC complexes. All compounds were characterized using physicochemical and spectroscopic techniques. Single-crystal X-ray diffraction study reveals a binuclear structure for one of the complexes and a mononuclear one for two others. These complexes exist as cationic Ag(I)–NHC complexes with the chelation of carbene carbons to the silver centre in an almost linear manner. The compounds were screened for their anti-bacterial activities against *Staphylococcus aureus* (ATCC 12600) as a Gram-positive bacterium and *Escherichia coli* (ATCC 25922) as a Gram-negative bacterium. The results show that both bacteria appear markedly inhibited. Furthermore, the results suggest the possibility of steric variation as a modulation of the anti-bacterial activities. The nuclease activities of the compounds were assessed using gel electrophoresis and the results indicate that these complexes can cleave or degrade DNA and RNA via a non-oxidative mechanism. Copyright © 2014 John Wiley & Sons, Ltd.

Additional supporting information may be found in the online version of this article at the publisher's web-site.

Keywords: Ag(I)–NHC complex; anti-bacterial activity; DNA cleavage; *N*-heterocyclic carbene; X-ray diffraction

Introduction

Imidazole- and benzimidazole-derived *N*-heterocyclic carbene (NHC) precursors are established compounds in the field of organometallic chemistry. Although imidazole-based derivatives could be the first NHC precursors to have been used by organometallic chemists, transition metal complexes of benzimidazole-derived NHCs have a robust history in catalysis and pharmacology.[1,2] Azoles (imidazole, benzimidazole, triazole, etc.) are heterocyclic compounds possessing a wide spectrum of biological activities, especially benzimidazole.[3–10] The biological relevance of benzimidazole-derived compounds is due to their structural similarity to the naturally occurring nucleotides, which facilitate their interaction with biopolymers of living systems.[11] Benzimidazoles, their derivatives and transition metal complexes have received considerable attention in coordination chemistry due to their well-documented biological activities. It has been found that such complexes show greater anti-microbial activities than the free ligands.[12,13] However, their interaction with biological systems requires appropriate selection of metals. Silver salts have a long-standing history as important therapeutic agents for maintaining human health. The effective use of silver for purification of drinking water, wound dressings for the promotion of healing and the prevention of eye infections in newborns is well established.[14–16] However, it is the low toxicity of silver salts for humans that has generated interest to further explore their biomedical applications, specifically anti-microbial and anti-cancer applications.[14,17–20] The coupling of these biologically compatible moieties generates a pharmaceutically enhanced class of compounds known as Ag(I)–NHC complexes.

Anti-microbial properties of Ag(I)–NHC complexes have been the subject of investigation.[21–23] Inspired by our previous research on the anti-cancer potential of benzimidazole-based binuclear Ag(I)–NHC complexes[24,25] and due to the fact that several studies have demonstrated the promising biological applications of binuclear complexes of both functionalized and non-functionalized NHCs as potent anti-cancer/anti-microbial agents against a variety of pathogens.[26] the current work is an effort to further explore this area of research. However, comparative investigation of the anti-bacterial activities of mononuclear and binuclear Ag(I)–NHC complexes is scarce. Hence, benzimidazolium salts were synthesized either with bromide or hexafluorophosphate counter anions and were further bonded with silver metal ions to yield mononuclear and binuclear Ag(I)–NHC complexes in order to compare their anti-bacterial potential against *Staphylococcus aureus* and

* *Correspondence to: Rosenani A. Haque, School of Chemical Sciences, Universiti Sains Malaysia, 11800 USM, Penang, Malaysia. E-mail: rosenani@usm.my*

a *School of Chemical Sciences, Universiti Sains Malaysia, 11800 USM, Penang, Malaysia*

b *Centre for Nano and Material Sciences, Jain University, Jain Global Campus, Bangalore 562112, Karnataka, India*

Escherichia coli bacteria. The bromide salts were moisture sensitive, and hence were converted to their more stable hexafluorophosphate counterparts by simple anion exchange reactions. These compounds were evaluated for their nuclease activity in the absence of an oxidizing agent in order to evaluate their self-activating properties which do not depend on the presence of co-reactants.

Experimental

Materials, Methods and Instrumentation

All chemicals were used as received. All solvents were redistilled except for acetonitrile and dimethylsulfoxide, which were of AR grade. NMR spectra were recorded with a Bruker 500 MHz spectrometer at room temperature in DMSO-d_6, using tetramethylsilane as an internal standard. FT-IR spectra were recorded with a PerkinElmer 2000 system FT-IR spectrophotometer in the range 400–4000 cm^{-1}. Elemental analysis was carried out with a PerkinElmer series II 2400 microanalyser. Melting points were measured using a Stuart Scientific SMP-1 (UK) instrument. Crystals were mounted on fine glass fibre or metal pin using viscous hydrocarbon oil. Data were collected with a Bruker-Smart ApexII-2009 CCD diffractometer, equipped with graphite monochromated Mo Kα (λ =0.71073 Å). Data collection temperatures were maintained at 100 K using open-flow nitrogen cryostreams. Integration was carried out with the SAINT program using APEX^{II} software.[27] Solutions were obtained by direct methods using SHELXS97, followed by successive refinements using full-matrix least-squares methods against F^2 using SHELXL97.[28] The X-seed program was used as graphical SHELX interface.[29] For compound **7**, the electron density around one of the allyl groups was modelled as disordered allyl chain over two positions (C45, C45A, C46 and C46A) with occupancies refined against each other (46:54%). Hydrogen atoms in one of disordered arms could not be located in Fourier difference map and were not included in the model. DFIX and DANG commands were used to model the observed disorder. The crystal contained significant pores with disordered solvent that could not be satisfactorily refined. However, the overall structure was not affected by this minor component as shown by other spectroscopy data (discussed below). The crystal data and structure refinement details for compounds **7–9** are summarized in Table 1.

Synthesis of Benzimidazolium Salts

*Synthesis of 1,1-diallyl-3,3-ethylenedibenzimidazolium dibromide (**1**)*

A mixture of benzimidazole (2.00 g, 16.93 mmol) and KOH (1.43 g, 25.40 mmol) in DMSO (20 ml) was stirred for 1 h at room temperature. 1,3-Dibromoethane (1.59 g, 8.46 mmol) was added portionwise and the mixture stirred at room temperature for 2 h. The mixture was poured into water (300 ml) and was cooled in ice; the resulting white precipitate was filtered, washed with water (4 × 5 ml) and dried in an oven at 70 °C. The compound obtained, 1,3-bis(*N*-benzimidazole)ethane (1.00 g, 3.80 mmol), was further reacted with allyl bromide (0.92 g, 7.60 mmol) in acetonitrile (35 ml) and refluxed at 80 °C for 20 h. The solvent was removed under reduced pressure to give **1** as a white solid. Recrystallization from methanol gave a crystalline solid. Yield 1.10 g (56%); m.p. 180–182 °C. ^{1}H NMR (500 MHz, DMSO-d_6, 298 K, δ, ppm): 4.85 (s, 4H, 2 × N–CH_2); 5.20 (d, J =6.0 Hz, 4H, 2 × N–CH_2–CH); 5.40 (dd, 2H, $^2J_{HH}$ =1.6 Hz, $^3J_{HH}$ =10.0 Hz, CH=HH_{cis}); 5.47 (dd, 2H, $^2J_{HH}$ =1.6 Hz, $^3J_{HH}$ =17.5 Hz, CH=CHH_{trans}); 6.10 (m, 2H, 2 × CH); 7.67 (d, J =8.0 Hz, 2H, benzimidazolium-H6) 7.69 (d, J =8.0 Hz, 2H, benzimidazolium-H7); 7.96 (t, J =8.0 Hz, 2H, benzimidazolium-H8); 8.10 (t, J =8.0 Hz, 2H, benzimidazolium-H9); 10.00 (s, 2H, 2 × NC*H*N). ^{13}C{^{1}H} NMR (125 MHz, DMSO-d_6, 298 K, δ, ppm): 30.7 (N–CH_2–CH_2); 44.0 (N–CH_2); 49.0 (N–CH_2-CH); 53.4 (–CH=CH_2); 114.1

Table 1. Crystal data and structure refinement details for compounds **7–9**

	7	**8**	**9**
Formula	$C_{46}H_{48}Ag_2F_{12}N_8P_2$	$C_{24}H_{28}AgF_6N_4P$	$C_{28}H_{32}AgF_6N_6P$
Formula weight	1218.60	625.34	705.44
Crystal system	Triclinic	Monoclinic	Monoclinic
Space group	*P*-1	*C*2/*c*	*C*2/*c*
a (Å)	12.7155(1)	9.5929(2)	14.6491(14)
b (Å)	13.0725(1)	17.7426(4)	16.2112 (15)
c (Å)	16.5597(2)	15.5410(3)	12.4226(15)
α (°)	96.990(1)	90	90
β (°)	105.149(1)	102.013(1)	93.228(1)
γ (°)	90.715(1)	90	90
V (Å^3)	2634.39(4)	2587.20(9)	2945.4(5)
Z	2	4	4
ρ_{cal} (g cm^{-3})	1.536	1.605	1.591
μ (mm^{-1})	0.886	0.905	0.806
Crystal size (mm)	0.08 × 0.24 × 0.30	0.21 × 0.27 × 0.67	0.07 × 0.12 × 0.29
Reflections measured	57739	18259	16291
Reflections unique	15269	4639	4179
R(int)	0.073	0.022	0.045
Reflections with $I \geq 2\,s(I)$	9683	4104	3233
θ range (°)	1.8–30.01	2.3–32.6	1.9–29.7
R ($I \geq 2\,s(I)$)	0.063	0.058	0.057
wR_2 (all data)	0.127	0.164	0.151
S	1.01	1.04	1.06

(benzimidazolium-*C*H6); 120.3 (benzimidazolium-*C*H7); 126.2 (benzimidazolium-*C*H8); 130.9 (benzimidazolium-*C*H9); 140.4 (NCHN). FT-IR (KBr disc, cm^{-1}): 3087, 3000 (C–H_{Ar}); 2990, 2995 ν(C–H_{aliph}); 1189, 1229 (C–N_{Ar}); 1691 (C=C, allyl). Anal. Calcd for $C_{22}H_{24}Br_2N_4$ (%): C, 52.38; H, 4.76; N, 11.11. Found (%): C, 52.69; H, 4.20; N, 11.42.

*Synthesis of 1,1-diallyl-3,3-propylenedibenzimidazolium dibromide (**2**)*

Salt **2** was prepared according to the same procedure as **1**, except that 1,2-dibromoethane was replaced by 1,3-dibromopropane (1.71 g, 8.46 mmol). Compound **2** was isolated as a white solid. Yield 1.25 g (63%); m.p. 187–189 °C. ^{1}H NMR (500 MHz, DMSO-d_6, 298 K, δ, ppm): 2.68 (br quint, J =7.0 Hz, 2H, N–CH_2–CH_2); 4.85 (t, J =7.0 Hz, 4H, 2 × N–CH_2); 5.20 (d, J =6.0 Hz, 4H, 2 × N–CH_2–CH); 5.38 (dd, 2H, $^2J_{HH}$ =1.6 Hz, $^3J_{HH}$ =10.0 Hz, CH=HH_{cis}); 5.45 (dd, 2H, $^2J_{HH}$ =1.6 Hz, $^3J_{HH}$ =17.5 Hz, CH=CHH_{trans}); 6.10 (m, 2H, 2 × CH); 7.63 (d, J =8.0 Hz, 2H, benzimidazolium-H6); 7.79 (d, J =8.0 Hz, 2H, benzimidazolium-H7); 7.99 (t, J =8.0 Hz, 2H, benzimidazolium-H8); 8.20 (t, J =8.0 Hz, 2H, benzimidazolium-H9); 10.05 (s, 2H, 2 × NC*H*N). ^{13}C{^{1}H} NMR (125 MHz, DMSO-d_6, 298 K, δ, ppm): 30.7 (N–CH_2–CH_2); 44.0 (N–CH_2); 51.2 (–CH=CH_2); 114.1 (benzimidazolium-*C*H6); 120.3 (benzimidazolium-*C*H7); 126.2 (benzimidazolium-*C*H8); 130.9 (benzimidazolium-*C*H9); 141.5 (NCHN). FT-IR (KBr disc, cm^{-1}): 3087, 3000 (C-H_{Ar}); 2990, 2995 ν (C-H_{aliph}); 1189, 1229 (C-N_{Ar}); 1691 (C=C, allyl). Anal. Calcd for $C_{23}H_{26}Br_2N_4$ (%): C, 53.28; H, 5.02; N, 10.81. Found (%): C, 53.67; H, 5.35; N, 11.19.

*Synthesis of 1-ethyl-3-allylbenzimidazolium hexafluorophosphate (**3**)*

KOH (1.85 g, 12.69 mmol) was added to a stirring solution of benzimidazole (1.00 g, 8.46 mmol) in DMSO (20 ml). The mixture was stirred for 1 h at room temperature and bromoethane (0.92 g, 8.46 mmol) was added dropwise. After 2 h the mixture was poured into water (300 ml) and extracted with chloroform (3 × 30 ml). The extract was filtered through four plies of Whatman filter papers in order to dry it. This process of filtration was repeated twice to collect a clear solution of the desired compound, which was evaporated under reduced pressure to give thick colourless oil. The compound formed, *N*-ethylbenzimidazole (1.00 g, 6.84 mmol), was added dropwise in a stirring solution of allyl bromide (0.82 g, 6.84 mmol) in acetonitrile (30 ml) and refluxed for 20 h. The solvent was removed under reduced pressure to give 1-ethyl-3-allylbenzimidazolium bromide which was then reacted with a solution of KPF_6 (1 equiv.) in methanol (20 ml). The mixture was stirred at room temperature for 3 h and allowed to stand overnight. The solvent was removed under reduced pressure and the resultant white powder was washed with distilled water (3 × 5 ml) to remove unreacted KPF_6, and air dried. The powder was recrystallized from a solution of acetonitrile–methanol to obtain a crystalline solid. Yield 1.10 g (60%); m.p. 126–128 °C. ^{1}H NMR (500 MHz, DMSO-d_6, 298 K, δ, ppm): 1.40 (t, J =7.0 Hz, 3H, CH_3); 4.58 (q, J =7.0 Hz, 2H, N–CH_2-CH_3); 5.22 (d, J =6.0 Hz, 2H, N–CH_2–CH); 5.36 (dd, 1H, $^2J_{HH}$ =1.5 Hz, $^3J_{HH}$ =10.2 Hz, CH=HH_{cis}); 5.45 (dd, 1H, $^2J_{HH}$ =1.5 Hz, $^3J_{HH}$ =17.2Hz, CH=CHH_{trans}); 6.06 (m, 1H, CH); 7.59–7.72 (m, 2H, benzimidazolium-H6/H7); 7.99–8.04 (m, 1H, benzimidazolium-H8); 8.06–8.18 (m, 1H, benzimidazolium-H9); 10.10 (s, 1H, NC*H*N). ^{13}C{^{1}H} NMR (125 MHz, DMSO-d_6, 298 K, δ, ppm): 48.7 (N–CH_2–CH); 52.6 (–CH=); 113.8 (benzimidazolium-*C*H6); 120.3 (benzimidazolium-*C*H7); 126.2 (benzimidazolium-*C*H8); 130.9 (benzimidazolium-*C*H9); 142.5 (NCHN). FT-IR (KBr disc, cm^{-1}): 3028 (C–H_{Ar}); 2991 (C–H_{aliph}); 1196 (C–N_{Ar}); 1661 (C=C, allyl). Anal. Calcd for $C_{12}H_{15}F_6N_2P$ (%): C, 43.43; H, 4.53; N, 8.43. Found (%): C, 42.53; H, 4.71; N, 8.45.

*Synthesis of 1-cyanopropyl-3-allylbenzimidazolium bromide (**4**)*

A mixture of benzimidazole (1.60 g, 13.50 mmol) and KOH (1.14 g, 20.25 mmol) in DMSO (20 ml) was stirred for 1 h at room temperature and 4-bromobutyronitrile (2.00 g, 13.50 mmol) was then added dropwise. After 2 h the mixture was poured into water (300 ml) and extracted with chloroform (3 × 30 ml). The extract was filtered thrice through four plies of Whatman filter papers to get a clear solution of the desired compound. The solvent was evaporated under reduced pressure to collect a thick fluid. The compound formed, *N*-cyanopropylbenzimidazole (0.60 g, 3.40 mmol), was added dropwise in a stirring solution of allyl bromide (0.40 g, 3.40 mmol) in acetonitrile (30 ml) and refluxed for 20 h. The solvent was removed under reduced pressure to give 1-cyanopropyl-3-allylbenzimidazolium bromide as a white solid. Yield 0.7 g (61%); m.p. 128–130 °C. ^{1}H NMR (500 MHz, DMSO-d_6, 298 K, δ, ppm): 2.35 (m, 2H, CH_2–CH_2–CN); 2.80 (t, J =7.0 Hz, 2H, CH_2–CN); 4.70 (t, J =7.0 Hz, 2H, N–CH_2–CH_2–CH_2–CN); 5.25 (d, J =6.0 Hz, 2H, N–CH_2–CH); 5.43 (dd, 1H, $^2J_{HH}$ =1.5 Hz, $^3J_{HH}$ =10.2 Hz, CH=HH_{cis}); 5.53 (dd, 1H, $^2J_{HH}$ =1.5 Hz, $^3J_{HH}$ =17.0 Hz, CH=CHH_{trans}); 6.10-6.20 (m, 1H, CH); 7.65–7.78 (m, 2H, benzimidazolium-H6/H7); 7.90–8.05 (m, 1H, benzimidazolium-H8); 8.10-8.18 (m, 1H, benzimidazolium-H9); 10.05 (s, 1H, NC*H*N). ^{13}C{^{1}H} NMR (125 MHz, DMSO-d_6, 298 K, δ, ppm): 30.3 (CH_2–C≡N); 44.0 (N–CH_2); 51.7 (N–CH_2–CH); 53.2 (–CH=); 116.5 (C≡N); 118.2 (benzimidazolium-*C*H6); 121.5 (benzimidazolium-*C*H7); 127.7 (benzimidazolium-*C*H8); 131.9 (benzimidazolium-*C*H9); 145.5 (NCHN). FT-IR (KBr disc, cm^{-1}): 3048 (C–H_{Ar}); 2996 (C–H_{aliph}); 1299 (C–N_{Ar}); 1661 (C=C, allyl); 2237 (C≡N). Anal. Calcd for $C_{14}H_{16}BrN_3$ (%): C, 54.92; H, 5.24; N, 13.72. Found (%): C, 55.32; H, 5.64; N, 14.15.

*Synthesis of 1-pentyl-3-allylbenzimidazolium hexafluorophosphate (**5**)*

Salt **5** was prepared according to the same procedure as **3**, except that bromoethane was replaced by 1-bromopentane (1.28 g, 8.46 mmol). Compound **5** was isolated as a pale brown solid. Yield 0.65 g (65%); m.p. 147–149 °C. ^{1}H NMR (500 MHz, DMSO-d_6, 298 K, δ, ppm): 0.86 (t, J =7.0 Hz, 3H, CH_3); 1.15 (m, 2H, CH_2–CH_3); 1.30 (m, 2H, CH_2–CH_2–CH_3); 1.90 (m, 2H, N-CH_2–CH_2); 4.55 (t, J =7.0 Hz, 2H, N–CH_2–R); 5.25 (d, J =6.0 Hz, 2H, N–CH_2–CH); 5.37 (dd, 1H, $^2J_{HH}$ =1.2 Hz, $^3J_{HH}$ =11.0 Hz, CH=HH_{cis}); 5.45 (dd, 1H, $^2J_{HH}$ =1.2 Hz, $^3J_{HH}$ =17.0 Hz, CH=CHH_{trans}); 6.00–6.13 (m, 1H, CH); 7.59–7.72 (m, 2H, benzimidazolium-H6/H7); 7.93–8.04 (m, 1H, benzimidazolium-H8); 8.06–8.18 (m, 1H, benzimidazole-H9); 10.10 (s, 1H, NC*H*N). ^{13}C{^{1}H} NMR (125 MHz, DMSO-d_6, 298 K, δ ppm): 14.9 (CH_3); 23.7 (CH_2), 29.3 (CH_2); 43.0 (N–CH_2); 50.7 (N–CH_2–CH); 52.6 (–CH=); 113.8 (benzimidazolium-*C*H6); 120.3 (benzimidazolium-*C*H7); 126.2 (benzimidazolium-*C*H8); 130.9 (benzimidazolium-*C*H9); 140.8 (NCHN). FT-IR (KBr disc, cm^{-1}): 3028 (C–H_{Ar}); 2979, (C–H_{aliph}); 1196 (C–N_{Ar}); 1659 (C=C, allyl). Anal. Calcd for $C_{15}H_{21}F_6N_2P$ (%): C, 48.12; H, 5.61; N, 7.48. Found (%): C, 48.63; H, 5.84; N, 7.46.

Synthesis of Ag(I)–NHC Complexes

*Synthesis of 1,1-diallyl-3,3-ethylenedibenzimidazolium disilver(I) bis(hexafluoro phosphate) (**6**)*

A mixture of **1** (0.60 g, 1.20 mmol) with Ag_2O (0.55 g, 2.40 mmol) in methanol (50 ml) was stirred at room temperature for 24 h. The reaction mixture was filtered through Celite to remove unreacted silver, and the solvent was removed under reduced pressure to yield Ag(I)–NHC dibromide complex, which was then reacted with a solution of KPF_6 (2 equiv.) in methanol (20 ml). The mixture was stirred

at room temperature for 3 h and allowed to stand overnight. Then the solvent was removed under reduced pressure and the resultant beige powder was washed with distilled water (3 × 5 ml) to remove unreacted KPF_6, and air dried. The product formed was collected and washed with diethyl ether to produce a fine, pale beige solid. Recrystallization from acetonitrile gave a crystalline solid. Yield 1.25 g (67%); m.p. 221–223 °C. ^{1}H NMR (500 MHz, DMSO-d_6, 298 K, δ, ppm): 4.80 (s, 8H, 4 × N–CH_2); 5.10 (d, J =6.0 Hz, 8H, 4 × N–CH_2–CH) 5.40 (dd, 4H, $^2J_{HH}$ =1.6 Hz, $^3J_{HH}$ =10.0 Hz, CH=HH_{cis}); 5.47 (dd, 4H, $^2J_{HH}$ =1.6 Hz, $^3J_{HH}$ =17.5 Hz, CH=CHH_{trans}); 6.00 (m, 4H, 4 × CH); 7.44 (d, J =8.0 Hz, 4H, benzimidazolium-H6); 7.45 (d, J =8.0 Hz, 4H, benzimidazolium-H7); 7.82 (t, J =8.0 Hz, 4H, benzimidazolium-H8); 7.90 (t, J =8.0 Hz, 4H, benzimidazolium-H9). ^{13}C{^{1}H} NMR (125 MHz, DMSO-d_6, 298 K, δ, ppm): 30.7 (N–CH_2–CH_2); 44.0 (N–CH_2); 49.0 (N–CH_2–CH); 53.4 (–CH=CH_2); 110.5 (benzimidazolium-*C*H6); 117.2 (benzimidazolium-*C*H7); 124.8 (benzimidazolium-*C*H8); 128.7 (benzimidazolium-*C*H9); 188.4 (C2 –Ag). FT-IR (KBr disc, cm^{-1}): 3219, 3125 (C–H_{Ar}); 2991, 2945 (C–H_{aliph}); 1350, 1464, 1465, 1485 (C–N_{Ar}); 1691 (C=C, allyl). Anal. Calcd for $C_{44}H_{44}Ag_2F_{12}N_8P_2$ (%): C, 44.36; H, 3.69; N, 9.41. Found (%): C, 44.67; H, 3.97; N, 9.71.

*Synthesis of 1,1-diallyl-3,3-propylenedibenzimidazolium disilver(I) bis(hexafluorophosphate) (**7**)*

Complex **7** was prepared according to the same procedure as **6**, except that **1** was replaced with **2** (0.68 g, 0.96 mmol) and Ag_2O (0.44 g, 1.92 mmol). Single crystals suitable for X-ray analysis were obtained by the slow diffusion of diethyl ether into acetonitrile solution containing the complex. Yield 1.35 g (70%); m.p. 225–227 °C. ^{1}H NMR (500 MHz, DMSO-d_6, 298 K, δ, ppm): 2.68 (br quint, J =7.0 Hz, 4H, 2 × N–CH_2–CH_2); 4.80 (t, J =7.0 Hz, 8H, 4 × N–CH_2); 5.10 (d, J =6.0. Hz, 8H, 4 × N–CH_2–CH); 5.38 (dd, 4H, $^2J_{HH}$ =1.6 Hz, $^3J_{HH}$ =10.0 Hz, CH=HH_{cis}); 5.45 (dd, 4H, $^2J_{HH}$ =1.6 Hz, $^3J_{HH}$ =17.5 Hz, CH=CHH_{trans}); 5.95 (m, 4H, 4 × CH); 7.44 (d, J =8.0 Hz, 4H, benzimidazolium-H6); 7.45 (d, J =8.0 Hz, 4H, benzimidazolium-H7); 7.79 (t, J =8.0 Hz, 4H, benzimidazolium-H8); 8.10 (t, J =8.0 Hz, 4H, benzimidazolium-H9). ^{13}C{^{1}H} NMR (125 MHz, DMSO-d_6, 298 K, δ, ppm): 30.7 (N–CH_2–CH_2); 44.0 (N–CH_2); 51.2 (–CH=CH_2); 110.5 (benzimidazolium-*C*H6); 117.2 (benzimidazolium-*C*H7); 124.8 (benzimidazolium-*C*H8); 128.7 (benzimidazolium-*C*H9); 189.8 (C2′–Ag). FT-IR (KBr disc, cm^{-1}): 3029, 3125 (C–H_{Ar}); 2991, 2945 (C–H_{aliph}); 1396, 1449, 1457, 1488 (C–N_{Ar}); 1694 (C=C, allyl). Anal. Calcd for $C_{46}H_{48}Ag_2F_{12}N_8P_2$ (%): C, 45.32; H, 3.94; N, 9.19. Found (%): C, 45.71; H, 4.32; N, 9.47.

*Synthesis of 1-ethyl-3-allylbenzimidazolium silver(I) hexafluorophosphate (**8**)*

To a suspension of **3** (0.80 g, 2.97 mmol) in acetonitrile (40 ml) was added Ag_2O (0.69 g, 2.97 mmol). The mixture was stirred at 50–60 °C for 12 h with the exclusion of light. The obtained grey solution was filtered through a pad of Celite and the filtrate was slowly evaporated to precipitate the required product. The compound was further purified by acetonitrile–dichloromethane to give a crystalline solid. Single crystals suitable for X-ray analysis were obtained by the slow diffusion of diethyl ether into acetonitrile solution containing the complex. Yield 1.12 g (75%); m.p. 185–187 °C. ^{1}H NMR (500 MHz, DMSO-d_6, 298 K, δ, ppm): 1.50 (t, J =7.0 Hz, 6H, 2 × CH_3); 4.60 (q, J =7.0 Hz, 4H, 2 × N–CH_2–CH_3); 5.22 (d, J =6.0 Hz, 4H, 2 × N–CH_2–CH); 5.36 (dd, 2H, $^2J_{HH}$ =1.5 Hz, $^3J_{HH}$ =10.2 Hz, CH=HH_{cis}); 5.45 (dd, 2H, $^2J_{HH}$ =1.5 Hz, $^3J_{HH}$ =17.2 Hz, CH=CHH_{trans}); 6.02 (m, 2H, 2 × CH); 7.50–7.65 (m, 4H, benzimidazolium-H6/H7); 7.77–7.86 (m, 2H, benzimidazolium-H8); 7.90–8.00 (m, 2H, benzimidazolium-H9). ^{13}C{^{1}H} NMR (125 MHz, DMSO-d_6, 298 K, δ, ppm): 48.7 (N–CH_2–CH); 50.7 (–CH=); 112.5 (benzimidazolium-*C*H6); 118.3 (benzimidazolium-*C*H7); 121.2 (benzimidazolium-*C*H8); 127.9 (benzimidazolium-*C*H9); 187.97, 190.56 ((d, ^1J(C–^{109}Ag) =209.5 Hz and d, ^1J(C–^{107}Ag) =181.0 Hz). FT-IR (KBr disc, cm^{-1}): 3117, 3005 (C–H_{Ar}); 2984, 2957 (C–H_{aliph}); 1390, 1439 (C–N_{Ar}); 1661 (C=C, allyl). Anal. Calcd for $C_{24}H_{28}AgF_6N_4P$ (%): C, 46.08; H, 4.48; N, 8.96. Found (%): C, 46.42; H, 4.55; N, 9.21.

*Synthesis of 1-cyanopropyl-3-allylbenzimidazolium silver(I) hexafluorophosphate (**9**)*

A mixture of **4** (0.60 g, 1.96 mmol) and Ag_2O (0.45 g, 1.96 mmol) in dichloromethane (40 ml) was stirred at room temperature for 24 h. The reaction mixture was filtered through Celite to remove unreacted silver and the solvent was removed under reduced pressure, which was then reacted with a solution of KPF_6 (1 equiv.) in methanol (20 ml) The mixture was stirred at room temperature for 3 h and allowed to stand overnight. The solvent was removed under reduced pressure and the resultant white powder was washed with distilled water (3 × 5 ml) to remove unreacted KPF_6, and air dried. The compound was further purified by acetonitrile–dichloromethane to give a crystalline solid. Single crystals suitable for X-ray analysis were obtained by the slow diffusion of diethyl ether into acetonitrile solution containing the complex. Yield 0.7 g (61%); m.p. 191–193 °C. ^{1}H NMR (500 MHz, DMSO-d_6, 298 K, δ, ppm): 2.25 (m, 4H, 2 × CH_2–CH_2–CN); 2.60 (t, J =7.5 Hz, 4H, 2 × CH_2–CN); 4.70 (t, J =7.5 Hz, 4H, 2 × N–CH_2–CH_2–CH_2–CN); 5.25 (d, J =6.0 Hz, 4H, 2 × N–CH_2–CH); 5.30 (dd, 2H, $^2J_{HH}$ =1.5 Hz, $^3J_{HH}$ =10.2 Hz, CH=HH_{cis}); 5.35 (dd, 2H, $^2J_{HH}$ =1.5 Hz, $^3J_{HH}$ =17.0 Hz, CH=CHH_{trans}); 6.06 (m, 2H, 2 × CH); 7.60–7.72 (m, 4H, benzimidazolium-H6/H7); 7.87–8.00 (m, 2H, benzimidazolium-H8); 8.05–8.15 (m, 2H, benzimidazolium-H9). ^{13}C{^{1}H} NMR (125 MHz, DMSO-d_6, 298 K, δ, ppm): 30.3 (CH_2–C≡N); 44.0 (N–CH_2); 51.7 (N–CH_2–CH); 53.2 (–CH=); 116.5 (C≡N); 120.2 (=CH_2); 117.4 (benzimidazolium-*C*H6); 120.0 (benzimidazolium-*C*H7); 125.7 (benzimidazolium-*C*H8); 129.5 (benzimidazolium-*C*H9); 189.0 (C2′–Ag). FT-IR (KBr disc, cm^{-1}): 3105, 3042 (C–H_{Ar}); 2986, 2960 (C–H_{aliph}); 1396, 1459 (C–N_{Ar}); 1661 (C=C, allyl); 2237 (C≡N). Anal. Calcd for $C_{28}H_{30}AgF_6N_6P$ (%): C, 47.80; H, 4.37; N, 11.95. Found (%): C, 47.88; H, 4.74; N, 12.24.

*Synthesis of 1-pentyl-3-allylbenzimidazolium silver(I) hexafluorophosphate (**10**)*

To a suspension of **5** (0.50 g, 1.62 mmol) in acetonitrile (40 ml) was added Ag_2O (0.38 g, 1.62 mmol). The mixture was stirred at 50–60 °C for 12 h with the exclusion of light. The obtained solution was filtered through a pad of Celite and the filtrate was slowly evaporated to precipitate a greyish solid. The compound was further purified by acetonitrile–dichloromethane to give a crystalline solid. Compound **10** was isolated as a grey powder. Yield 0.62 g (65%); m.p. 201–203 °C. ^{1}H NMR (500 MHz, DMSO-d_6, 298 K, δ, ppm): 0.86 (t, J =7.0 Hz, 6H, 2 × CH_3); 1.15 (m, 4H, 2 × CH_2–CH_3); 1.30 (m, 4H, 2 × CH_2–CH_2–CH_3); 1.90 (m, 4H, 2 × N–CH_2–CH_2); 4.55 (t, J =7.0 Hz, 4H, 2 × N–CH_2–R); 5.25 (d, J =6.0 Hz, 4H, 2 × N–CH_2–CH); 5.30 (dd, 2H, $^2J_{HH}$ =1.2 Hz, $^3J_{HH}$ =11.0 Hz, CH=HH_{cis}); 5.39 (dd, 2H, $^2J_{HH}$ =1.2 Hz, $^3J_{HH}$ =17.0 Hz, CH=CHH_{trans}); 6.05 (m, 2H, 2 × CH); 7.50–7.65 (m, 4H, benzimidazolium-H6/H7); 7.77–7.86 (m, 2H, benzimidazolium-H8); 7.90–8.00 (m, 2H, benzimidazolium-H9). ^{13}C{^{1}H} NMR (125 MHz, DMSO-d_6, 298 K, δ, ppm): 14.90 (CH_3); 23.7 (CH_2); 29.3 (CH_2); 43.0 (N–CH_2); 50.7 (N–CH_2–CH); 55.6 (–CH=); 112.5 (benzimidazolium-*C*H6); 118.3 (benzimidazolium-*C*H7); 121.2 (benzimidazolium-*C*H8); 127.9 (benzimidazolium-*C*H9); 179.7, 180.6 ((d, ^1J(C–^{109}Ag) =199.5 Hz and d, ^1J(C–^{107}Ag) =185.0 Hz). FT-IR (KBr disc, cm^{-1}): *ca* 3100, 3045 ν(C–H_{Ar}); 2996, 2967 (C–H_{aliph});

1396, 1459 (C–N_{Ar}); 1661 (C=C, allyl). Anal. Calcd for $C_{30}H_{40}AgF_6N_4P$ (%): C, 50.77; H, 5.64; N, 7.92. Found (%): C, 51.16; H, 5.71; N, 7.89.

Anti-bacterial Studies

Stock solutions of all compounds were prepared using DMSO. Anti-bacterial tests were performed using the Kirby Beur disc diffusion method.[30] Single colonies of *E. coli* and *S. aureus* from fresh culture agar plates were, respectively, cultured in two bottles containing 5 ml of nutrient broth solution (Tryptone10 g, yeast extract 5 g, NaCl 10 g l^{-1}), and incubated overnight at 37 °C. The turbidity of each culture was adjusted by comparing it to 0.5 McFarland standard, which is equal to 1.58×10^8 CFU ml^{-1} or 0.5 (OD_{600} reading). Using sterile cotton buds, each bacterial lawn culture was spread uniformly on different agar plates before placing the anti-microbial assay discs on the plate. Five discs were placed on the agar plate and 5 μl volumes of the compounds, $AgNO_3$ and ciprofloxacin were loaded on the discs with concentrations at 100 and 50 μg ml^{-1}. The plates were incubated at 37 °C for 24 h. The diameters of the inhibition zones were measured in millimetres, which was calculated as a mean of three replicates. The effectiveness of these compounds in terms of inhibition zone was compared to silver nitrate based on its established anti-microbial properties[31] and ciprofloxacin which were used as positive controls. The minimum inhibitory concentration (MIC) of each compound was determined based on the lowest concentration of the compound that inhibited the growth of bacteria using the broth dilution method.[32] Single colonies of *S. aureus* and *E. coli* were isolated from agar plates and were grown in 5.0 ml of lysogeny broth (LB). The solutions were incubated at 37 °C for 24 h in a shaking incubator at 180 rpm to yield bacteria solutions. Stock solutions of the compounds were prepared by dissolving each in DMSO to prepare stock concentrations at 50 mg ml^{-1}. Respectively, from each stock solution, 2 μl of the compounds, $AgNO_3$ and ciprofloxacin were dissolved in 2 ml of the broth culture and used to prepare six serial dilutions of 100, 50, 25, 12.5, 6.25 and 3.125 μg ml^{-1}. Serial dilutions were done for each compound by transferring 1 ml (100 μg ml^{-1}) of the compound solution from the first tube to the second tube already containing 1 ml of nutrient broth. Next, 1 ml from tube 2 was again transferred into tube 3 and same was repeated for tubes 4, 5 and 6 to give concentrations of 100, 50, 25, 12.5, 6.25 and 3.125 μg ml^{-1} respectively. Prepared bacteria solution (5 μl) was added to the dilution series on a daily basis for five days and the tubes were incubated at 37 °C for 16 h in a shaking incubator at 180 rpm. Bacteria growth was noted by turbidity of the solution in the tubes and MIC was determined by the lowest concentration lacking turbidity.

Gel Electrophoresis

The electrophoresis method was employed to study the efficiency of cleavage by the test compounds.[33] The extracted plasmid DNA and RNA, pTS414 (10 μg ml^{-1}) and1 μl of the test compound (50 μg ml^{-1}) were mixed in 50 mM Tris-HCl buffer (pH =8.00). The contents were incubated for 8 h at 37 °C. Plasmid extraction was done using a plasmid purification kit (Intron Biotechnology, Korea) without the addition of RNase in order to extract both RNA and DNA. The electrophoresis was performed using 0.8% agarose gel. For each sample 5 μl of the mixture was loaded into the well. The voltage used was 90 V running on 0.5 × Tris-acetate EDTA buffer and the gel was stained with ethidium bromide solution (10 μg ml^{-1}) for 15 min. The gel was subsequently exposed to UV light and captured by a gel documentation system (FluorChem HD2, Cell Bioscience). The nucleating ability of the synthesized benzimidazolium salts/Ag–NHC complexes (**1–10**) was determined by their efficiency in cleaving/degrading the plasmid DNA and RNA.

Results and Discussion

Syntheses

Ag(I)–NHC complexes are known to assume diverse architectures, based on the reaction conditions employed. In the present study, we describe the preparations of NHC precursors (**1–5**) and their respective mononuclear/binuclear Ag–NHC complexes (**6–10**). The synthetic route to **1–5** is shown in Scheme 1. In the case of **1** and **2**, 1,3-bis(*N*-benzimidazole)ethane and 1,2-bis(*N*-benzimidazole) propane are formed from the deprotonation of benzimidazole with KOH and subsequent alkylation with 1,3-dibromoethane and 1,2-dibromopropane in DMSO to yield ethyl and propyl bridged architectures, respectively. Afterward, reactions with allyl bromide (2 equiv.) in acetonitrile afford, respectively, bis-benzimidazolium bromide (1,1-diallyl-3,3-ethylenedibenzimidazolium (**1**) and 1,1-diallyl-3,3-propylenedibenzimidazolium (**2**) dibromide) salts as white solids in good yield (Scheme 1). The benzimidazolium salts **3**, **4** and **5** were prepared from benzimidazole by stepwise alkylation with bromoethane, 4-bromobutyronitrile and 1-bromopropane, respectively, in the presence of KOH in DMSO at room temperature for 2 h. The reactants were subsequently converted into their respective quaternary salts by the reaction of allyl bromide, followed by treatment with KPF_6 in the case of **3** and **5** to obtain stabilized NHC salts (Scheme 1). Salts **1–5** are non-hygroscopic, stable to air and moisture, and soluble in common organic solvents such as DMF, DMSO, acetone and acetonitrile.

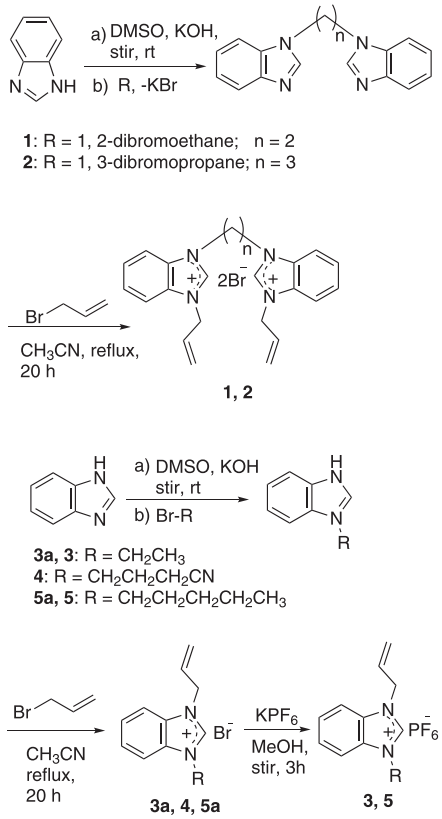

Scheme 1. Synthesis of bis- and mono-benzimidazolium salts (**1–5**).

Reactions of salts **1** and **2** with Ag_2O in a 2:1 molar ratio in methanol for 24 h gave binuclear Ag–NHC complexes. The so obtained bromide complexes were directly converted into their corresponding hexafluorophosphate counterparts by salt metathesis reaction using KPF_6 (2 equiv.) in methanol to afford respective bis (hexafluorophosphate) complexes **6** and **7** in good yield after recrystallization from acetonitrile–dichloromethane. Mononuclear complexes **8** and **10** were prepared in good yield by *in situ* deprotonation reactions of the corresponding hexafluorophosphate benzimidazolium salts with Ag_2O in a 1:1 molar ratio in acetonitrile at stirring conditions (50–60 °C) for 12 h and in methanol for 24 h at room temperature in the case of **9**. The mixture was filtered through a pad of Celite, and the filtrate was slowly evaporated to precipitate a white solid. The obtained solid was redissolved in acetonitrile and diethyl ether was added to reprecipitate the solid in pure form. Basic Ag_2O plays two important roles in this reaction. First, it serves as a base to deprotonate the imidazolium proton and generates the free NHC; second, it is a source of silver for metalation reaction. The efficiency of the Ag_2O route in the synthesis of the reported Ag(I)–NHC complexes is attributed to its higher proton affinity than the NHC salt. This involves a spontaneous deprotonation of the first NHC salt in the presence of CH_3CN, followed by a low barrier and also spontaneous metalation, leading to the formation of NHC–Ag^+–N≡C–CH_3 and AgOH. This is followed by the deprotonation of second NHC by AgOH by the formation of a strong C_{NHC}–H···OAg hydrogen bond.[34] After metalation, the second thermodynamically more stable $[Ag–(NHC)_2]^+$ is obtained as the final product. The Ag(I)–NHC complexes (**6–10**) are thermally stable up to their melting points and are non-hygroscopic. The complexes are readily soluble in DMSO, DMF and acetonitrile. Synthetic routes to the complexes are shown in Scheme 2.

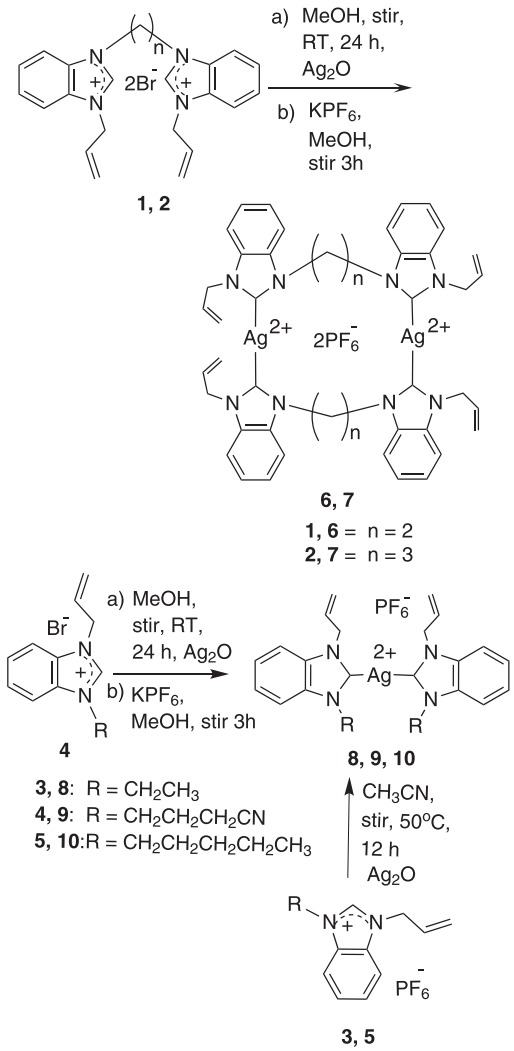

Scheme 2. Synthesis of Ag–NHC complexes (**6–10**).

Spectroscopic Studies

Solution studies of these complexes are essential in order to identify the bioactive species resulting from the dissolution of the solid complexes, and so understand the underlying biochemical mechanism involved in the anti-bacterial activity. This study is also relevant to anti-bacterial investigations since the complexes have to be maintained in culture medium for at least 24 h. Hence, we have determined the stabilities of the Ag(I)–NHC complexes in D_2O–10% DMSO-d_6 and 100% DMSO-d_6. All investigated Ag(I)–NHC complexes are stable in aqueous solution for 24 h, since their ^{1}H NMR and ^{13}C NMR spectra remain similar after 24 h. The ^{1}H NMR and ^{13}C NMR spectra of complex **8** after 24 h in 10% aqueous DMSO are shown in Figs S6–S9, and are identical to the spectra obtained after 15 min (see supporting information).

In order to further assess the stability of these Ag(I)–NHC complexes in the broth mixture, 10 mg ml^{-1} stock solutions of the complexes in DMSO were prepared and added in a 1:1 ratio to LB made in DMSO. This was done to imitate the conditions of the MIC evaluation experiments. The ^{1}H NMR and ^{13}C NMR spectra were taken after 15 min and 24 h. The complexes demonstrate stability in the LB/DMSO broth mixture at 37 °C, as shown by the unchanged ^{1}H NMR and ^{13}C NMR spectra after 24 h.

The FT-IR bands for the C–H stretching vibrations in both alkylbenzimidazoles and bis-benzimidazolium salts appear at around 2945–3100 cm^{-1}. FT-IR spectra of the salts show a band of medium intensity in the range 1185–1299 cm^{-1}, which is assigned to benzimidazole ring (C=N) vibrations. In the spectra of the complexes this band shows a positive shift of 115–120 cm^{-1}, indicating coordination of the benzimidazole ring.[35] Thus, it can be concluded that the binding of carbene carbon to silver ion strengthens the vibrations in the aforementioned range. A moderate band observed in the range 1660–1694 cm^{-1} is ascribed to the stretching vibration (C=C) of the allyl functionality in the carbene precursors[36] and remains unchanged in the carbene complex spectra. This is an indication that the allyl functionality is outside the coordination sphere of the coordinatively saturated Ag(I) centre.[37] Finally, a sharp band at around 2237 cm^{-1} is assigned to ν(C≡N) of the nitrile functionality.[38]

The ^{1}H NMR spectra of benzimidazolium salts **1–5** in DMSO-d_6 exhibit a characteristic NC*H*N proton resonance at *ca* 10.00–10.10 ppm, suggesting the successful formation of the desired salts. This is quite consistent with data for other benzimidazole-based NHC precursors.[38–40] The ^{1}H NMR spectra of all compounds display signals for the terminal hydrogen atoms of the allyl group at *ca* 4.36 and 4.53 ppm with typical J_{HH} coupling constants ($^3J_{HH}$ =10.2–11.0 Hz *cis* and $^3J_{HH}$ =17.0–17.2 Hz *trans*). In addition, the resonances of aliphatic protons of the alkyl chain are consistent in the range *ca* 0.86–4.50 ppm, which is in agreement with similar structures found in the literature.[41] In the ^{13}C NMR spectra, chemical shifts due to the C-2 carbon are observed in the range *ca* 140.4–145.5 ppm, which is in agreement with reported data

for similar benzimidazolium salts.[42–44] The signals for alkyl chain (–CH_2–) are observed at *ca* 10.00–49.87 ppm. As expected, in the ^{1}H NMR spectra of the complexes, the signal corresponding to the NC*H*N proton resonance is absent due to the loss of this acidic proton after reacting with Ag_2O. This suggest successful complex formation which is further confirmed by the appearance of a diagnostic silver-bound carbene (NCN–Ag) signal at *ca* 188.4, 189.8 and 189.0 ppm for complexes **6**, **7** and **9**, respectively in the ^{13}C NMR spectra. In the case of **8** and **10**, the ^{13}C NMR spectra display a downfield resonance pattern for the C2-carbon nuclei as two doublets centred at 187.9, 190.6 and 189.7, 191.6 ppm, respectively. This is due to the presence of ^{13}C–^{109}Ag and ^{13}C–^{107}Ag with coupling constants of ^1J(C–^{109}Ag) =209.5, ^1J(C–^{107}Ag) =181.0 and ^1J(C–^{109}Ag) =199.5, ^1J(C–^{107}Ag) =185.0 Hz, respectively. This observation is in accord with those of similar compounds.[41,45] Apart from these major changes, there are no observable changes observed in either spectra.[43,46,47]

Crystal Structures

Complex **7** crystallizes in a triclinic space group *P*-1 with the asymmetric unit containing one binuclear molecule, one full PF_6^- and two half PF_6^-, each located on a centre of inversion. The presence of two PF_6 anions in the lattice neutralizes the charge of the metal complex. Each of the Ag(I) centres is coordinated to two carbene carbon atoms of the ligand which display a μ-κ^1(C)Ag:κ^1(C′)Ag′ coordination mode (Fig. 1(a)). The distances between the metal centre and carbene carbon are in the range 2.079(4)–2.092(4) Å, which are close to the mean values found in comparable bis-benzimidazole complexes of Ag(I).[47–49] Both Ag(I) ions are in a two-coordinate distorted linear environment with angles 173.22(16)° for C1–Ag1–C24 and 171.89(19)° for C14–Ag2–C37. The internal ring angles of benzimidazole rings at the carbene centre are in the range 104.49(4)–106.25(4)°, which are in good agreement with those of reported complexes having a similar ligand architecture.[50–52] In the extended structure of **7**, the π–π interactions are observed between benzimidazole rings, either with face-to-face interactions or edge-to-face interactions (Fig. 1(b)). This results in the formation of a two-dimensional supramolecular network.

Complex **8** crystallizes in the monoclinic space group *C*2/*c* with half of the molecule comprising the asymmetric unit, having twofold symmetry (Fig. 2(a)). The central Ag(I) is coordinated to two carbene carbon atoms, giving the C1–Ag1–C1^i angle as 172.79(13)° (where $^i = -x, y, ½ - z$). The silver–carbene bond distance for Ag1–C1 is 2.085(3) Å. Face-to-face π–π interactions between two adjacent benzimidazole rings are observed with a distance of 3.559(7) Å. Overall this leads to the formation of a one-dimensional stepped chain network (Fig. 2(b)).

Complex **9** crystallizes in the monoclinic space group *C*2/*c*, with one half of the molecule in the asymmetric unit, having twofold symmetry (Fig. 3(a)). The central Ag(I) makes a linear coordination geometry through two carbene carbon atoms (C1–Ag1–C1^i) with a bond angle of 177.76(13)°. The Ag atom coordinates to two

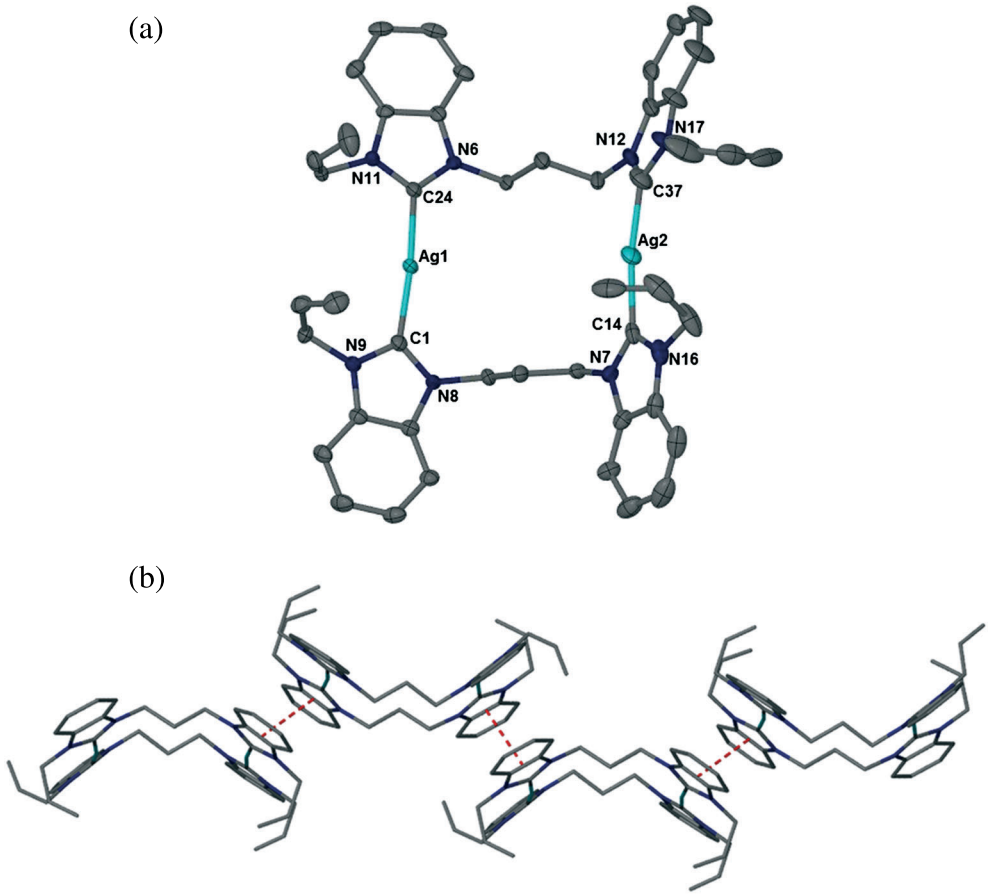

Figure 1. (a) Molecular structure of **7** with ellipsoids drawn at 50% probability. Hydrogen atoms and PF_6 anion in the lattice are omitted for clarity. Selected bond lengths (Å): Ag1–C1 = 2.079(4); Ag1–C24 = 2.092(4); Ag2–C14 = 2.091(5); Ag2–C37 = 2.083(6). Selected bond angles (°): N8–C1–N9 = 106.2(4); N7–C14–N16 = 106.2(4). (b) The π–π interactions (face-to-face) between benzimidazole rings.

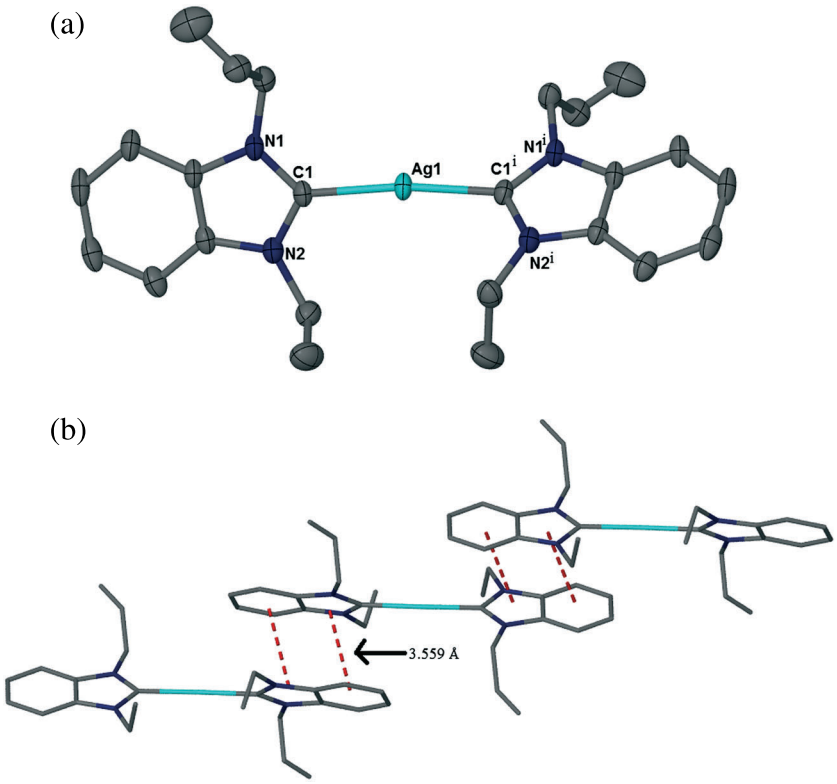

Figure 2. (a) Molecular structure of **8** with the ellipsoids drawn at 50% probability. Symmetry element used: $^{i} = -x, y, \frac{1}{2} - z$. Selected bond lengths (Å): C1–N1 = 1.350(4); C1–N2 = 1.395(4). Selected bond angle (°): N1–C1–N2 = 110.63(10). (b) Face-to-face π–π interactions between benzimidazole rings.

carbene groups with a distance of 2.089(8) Å for Ag1–C1 (and its equivalent geometry $C1^{i}$ in which $^{i} = -x - \frac{1}{2}, \frac{3}{2} - y, 1 - z$). The two coordinated benzimidazolium rings are perpendicular to each other with a dihedral angle of approximately 43°. The nitrile groups of the ligand are pointed directly to the Ag(I) ion in the adjacent molecule, resulting in the C11–N3–$Ag1^{i}$ angle of 178.16(8)°. The weak interactions between silver ions with nitrogen atom of nitrile groups, Ag1 ⋯ $N3^{i}$, is 3.516(9) Å (Fig. 3(b)). In the crystal packing, the PF_6 anions are observed to reside in the windows of the three-dimensional sheet in structure **9** (Fig. 3(c)).

Anti-bacterial Activities

Stock solutions of all compounds were prepared in DMSO. The concentrations of the test compounds were 3.125, 6.25, 12.5, 25, 50 and 100 μg ml^{-1}, using silver nitrate and ciprofloxacin (standard drug) as positive controls. In a solvent control test, the effect of 10% DMSO was studied on the growth of microorganisms, and no inhibitory activity was observed. Compounds were screened for their anti-bacterial activities against *E. coli* and *S. aureus* using the disc diffusion method. *S. aureus* and *E. coli* are common pathogenic species of Gram-positive and Gram-negative bacteria. They usually cause a range of infections responsible for many illnesses in humans. Gram-negative bacteria and Gram-positive bacteria differ significantly from each other in terms of structure. Gram-negative bacteria possess an outer cell membrane in addition to the cytoplasmic membrane found in Gram-positive bacteria. The extra cell membrane found in Gram-negative bacteria offers an additional protective barrier from the environment compared with Gram-positive bacteria. As a result, Gram-negative bacteria are usually more difficult to kill because they display more resistance against anti-microbial agents.[53] The result of the present study seems to confirm the foregoing, since the bacterial strains exhibit different susceptibilities to most of the test compounds. The susceptibility levels of the Gram-negative bacterium to the complexes are higher than those of the Gram-positive bacterium.

The MIC was determined based on the lowest concentration that inhibited the growth of the bacteria. Electron-donating or electron-withdrawing groups attached to the *N*-position of the benzimidazole ring were replaced to explore the anti-bacterial potency. All complexes in this study are effective at inhibiting the growth of *E. coli* and *S. aureus* bacteria. This is with the exception of complex **8** whose activity is not observed for *E. coli* at 50 μg ml^{-1}, while the corresponding salts are inactive against both strains of bacteria (Table 2). Among the test compounds, **6**, **7**, **9** and **10** exhibit significant activity against both bacterial strains. The MIC values of the complexes against both *E. coli* and *S. aureus* are in the range 12.5–100 μg ml^{-1} (Table 3). These complexes in comparison with silver nitrate have significantly better anti-bacterial qualities and comparable to some other related results in the literature, and in some cases, the complexes show better results,[19,50,52–55] indicating that these new Ag(I)–NHC complexes are quite potent. Complexes **6**, **7**, **9** and **10** show good to moderate bacteriostatic effect against *E. coli* at 25–50 μg ml^{-1}, while for complex **8** the activity is 100 μg ml^{-1}. These results show that **6** and **7** (binuclear silver complexes) are the most sensitive against both bacteria. These binuclear Ag(I)–NHC complexes (**6** and **7**) have relatively better anti-bacterial potential compared with their mononuclear counterparts (**8–10**), considering the fact that the number of Ag atoms in complexes **6** and **7** is twice that of complexes **8–10**. This further underscores the existing literature that the number of silver centres within a complex molecule determines its biological activities.[56] We found that, as the size of *N*-alkyl substituent on the complex increases, its anti-bacterial activity also increases, i.e. **8** < **9** < **10**,

Applied Organometallic Chemistry

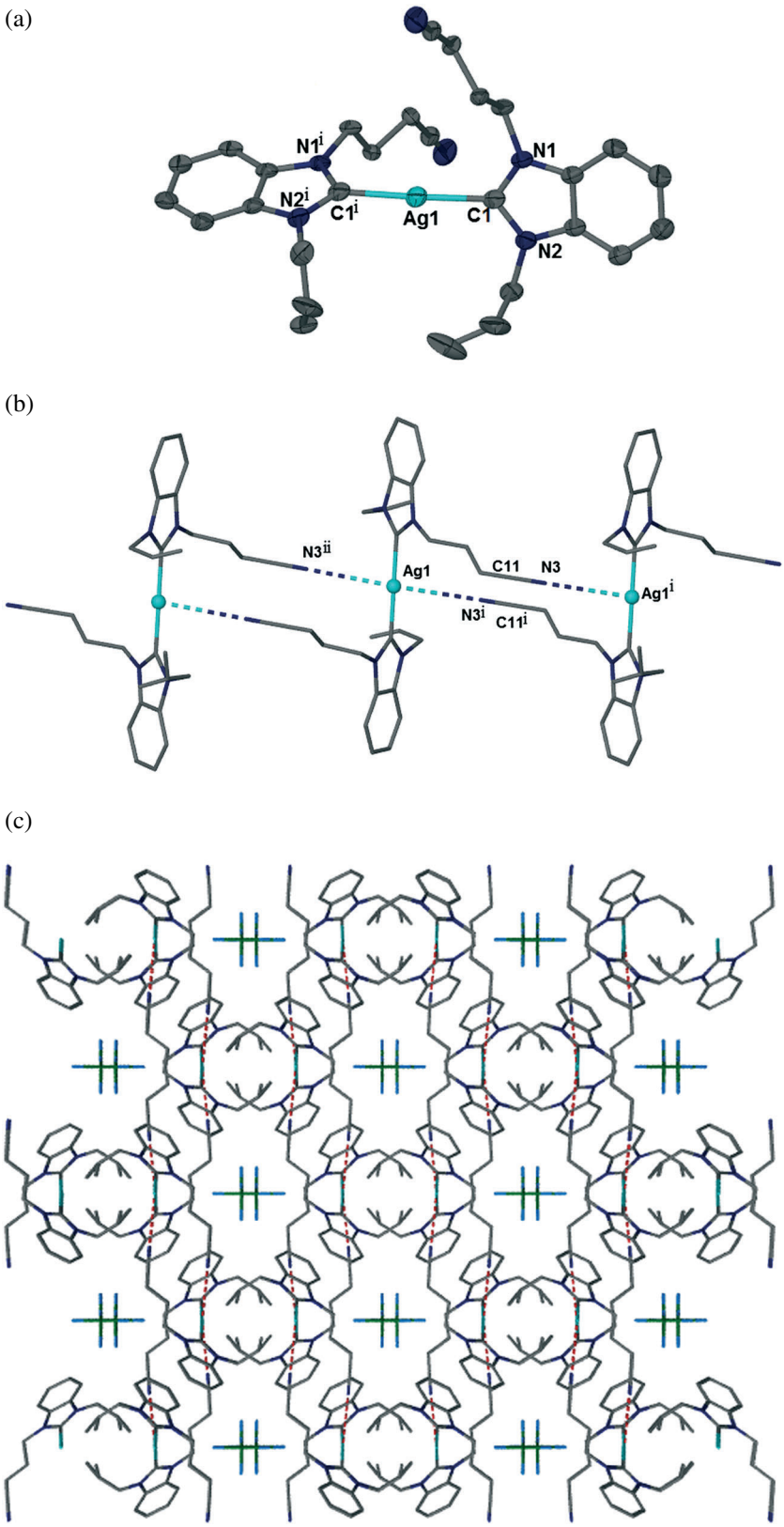

Figure 3. (a) Molecular structure of **9** with ellipsoids drawn at 50% probability. Hydrogen atoms and PF_6 anions are omitted for clarity. Selected bond lengths (Å): C1–N1 = 1.353(5), C1–N2 = 1.400(5). Selected bond angle (°): N1–C1–N2 = 111.15(3). (b) Ag···$N3^{i}$ interaction in crystal structure in **9**. Symmetry elements used: $^{i} = -x - \frac{1}{2}, \frac{3}{2} - y, 1 - z$; $^{ii} = \frac{1}{2} + x, \frac{3}{2} - y, \frac{1}{2} + z$. (c) View of three-dimensional network structure of **9** along *c*-axis.

showing that the type of substituent at the *N*-position has an effect on the anti-bacterial activity.[57,58] The anti-bacterial effect could be due to increased lipophilicity of the complexes because of the alkyl chain, which in turn facilitates the transport of Ag(I)–NHC complexes into the cell and thus might possibly cause toxicity by interfering with cellular respiration and metabolism of biomolecules.

Table 2. Anti-bacterial activities of the compounds[a] against *E. coli* and *S. aureus* obtained using the disc diffusion method[b] (zone of inhibition ± SD)

Test compound	Concentration ($\mu g\ ml^{-1}$)	Inhibition zone (mm)	
		E. coli	*S. aureus*
6	50	19.3 ± 0.5	20.7 ± 0.4
7	50	21.0 ± 0.8	21.5 ± 1.5
8	50	—	7.5 ± 0.4
9	50	14.7 ± 1	15.0 ± 2
10	50	15.0 ± 1	16.0 ± 4
$AgNO_3$	50	14.0 ± 3	15.5 ± 2
Ciprofloxacin	50	27.5 ± 1	27.5 ± 1
6	100	25.8 ± 2	26.3 ± 2
7	100	27.0 ± 4	28.2 ± 3
8	100	9.5 ± 1	14.5 ± 1
9	100	24.6 ± 1.5	25.0 ± 2
10	100	25.4 ± 0.7	25.4 ± 0.7
$AgNO_3$	100	20.3 ± 3	20.7 ± 1
Ciprofloxacin	100	333.4 ± 0.5	35.5 ± 0.5

[a]Compounds 1-5 showed no activity.
[b]Test compound volume =5 µl.

The data indicate that these complexes are more stable than $AgNO_3$ in the bacterial solution since the growth of bacteria treated with these complexes on a daily basis is delayed for a longer time (Table 3). The observed results can be explained by the slow decomposition of these Ag(I)–NHC complexes in the aqueous culture medium. Interestingly, the growth of bacteria is delayed further when treated with complex **9**, compared with the other complexes. This observation could be due to the presence of an electron-withdrawing nitrile functionality at the *N*-position of complex **9**. It was hypothesized that the σ-withdrawers and π-donators lead to a reduction of σ-donor capability,[59] thereby leaving the carbene carbon centre with less electron density and, therefore, less susceptible to attack by protons present in an aqueous environment. In all cases the complexes show good to moderate bacteriostatic effect against both bacterial strains.

Nuclease Activity

The interaction of plasmid pTS414 DNA/RNA with the test compounds was investigated using gel electrophoresis in the absence of an oxidant. Plasmid extraction was done using a plasmid purification kit (Intron Biotechnology, Korea) without the addition of RNase in order to extract both RNA and DNA. This method is intended to further investigate the interaction of the synthesized compounds with DNA and/or RNA as an initial experiment for studying likely mode of action(s) of the reported compounds. When circular plasmid is exposed to gel electrophoresis, the fastest migration is observed for the supercoil form (Form I). If scission occurs on one strand it is referred to as nicked circular (Form II). If both strands are cleaved, a linear form (Form III) that migrates between Form I and Form II will be generated.[60] Finally, the test compounds can also degrade the plasmid DNA and/or RNA.[61,62] The gel

Table 3. Minimum inhibitory concentration (MIC) against *E. coli* and *S. aureus* after addition of constant volume of bacterial solution on a daily basis

Test compound	MIC ($\mu g\ ml^{-1}$)		*E. coli*/*S. aureus*				
	E. coli	*S. aureus*	Day 1	Day 2	Day 3	Day 4	Day 5
6	25	12.5	×	×	×	×	√
7	25	12.5	×	×	×	×	√
8	100	100	×	×	√		
9	50	25	×	×	×	×	×
10	25	25	×	×	×	√	
$AgNO_3$	50	50	×	√			
Ciprofloxacin	6.25	6.25	×	×	×	×	×

Growth = √; no growth = ×.

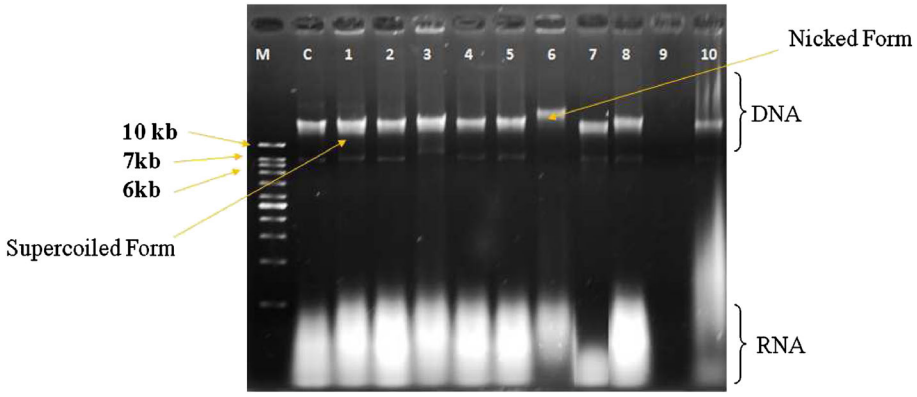

Figure 4. Nuclease activity (50 $\mu g\ ml^{-1}$). M: marker; C: DNA/RNA alone; lane 1: DNA/RNA +**1**; lane 2: DNA/RNA +**2**; lane 3: DNA/RNA +**3**; lane 4: DNA/RNA +**4**; lane 5: DNA/RNA +**5**; lane 6: DNA/RNA +**6**; lane 7: DNA/RNA+ **7**; lane 8: DNA/RNA +**8**; lane 9: DNA/RNA +**9**; lane 10: DNA/RNA +**10**.

electrophoresis images are shown in Fig. 4. In lane 2, DNA/RNA alone does not show any activity. All salts show no apparent interaction with nucleic acids, but, with the exception of complex **8**, the Ag(I)–NHC complexes exhibit cleavage activity. Complex **6** is able to convert supercoiled DNA (Form I) to the upper nicked form (Form II) and at the same time showing some degree of RNA degradation (lane 6). Complex **7** shows no visible activity towards DNA (lane 7); however, there is evidence of RNA degradation. Complexes **9** and **10** display distinct nuclease activities, especially complex **9**, which clearly degrades the nucleic acids, as can be seen in lane 7. Complex **9** is able to induce DNA double-strand cleavage without converting to the intermediate linear form of DNA; consequently it leads to complete DNA degradation. The plasmid DNA is totally degraded, leading to the loss of the associated bands on the gel.[61] The nuclease activity of **9** relative to the other analogues as evident from the complete degradation of DNA and RNA could be due to the presence of an electron-withdrawing group in the complex: the positive charge of the Ag ion increases, and this enhances the ability of the Ag ion to interact with DNA. This observation suggests that these Ag(I)–NHC complexes have potential to cleave nucleic acids by a non-oxidative mechanism, possibly by a hydrolytic path which has yet to be clarified conclusively.

Conclusions

A new series of NHC precursors and their corresponding Ag(I)–NHC complexes have been successfully synthesized and characterized and shown to exist as mononuclear and binuclear species. The binuclear structure of **7** and mononuclear structures of **8** and **9** were established using single-crystal X-ray diffraction techniques. These Ag–NHC complexes clearly showed superiority over silver nitrate, an established anti-microbial agent. This demonstrates the potential of these complexes as good candidates for the treatment of bacterial infections. The present work also suggest that binuclear Ag(I)–NHC complexes have better anti-bacterial potential compared with their mononuclear counterparts. The bacterial growth inhibition capacity followed the order: **7** > **6** > **10** > **9** > **8**. This study suggests that these complexes can be further explored as excellent anti-bacterial agents owing to their good activity against the studied bacterial strains. Complexes **6**, **7**, **9** and **10** show cleavage and degradation of DNA and RNA in the absence of co-reactants. Although the mechanism of anti-microbial activity of these complexes is not completely understood, it seems that the type of substituents at the *N*-position have an effect on anti-bacterial activity as evident from the results for complexes **8–10**. Further studies on this finding are in progress.

Acknowledgements

R. A. Haque thanks Universiti Sains Malaysia for Research University grant 1001/PKIMIA/811217. P. O. Asekunowo thanks IPS, USM for financial support (GA: PKD0004/12(R)).

References

[1] F. E. Hahn, L. Wittenbecher, R. Boese, D. Blaser, *Chem. Eur. J.* **1999**, *5*, 1931.
[2] F. E. Hahn, L. Wittenbecher, D. L. Van, R. Frohlich, *Angew. Chem. Int. Ed.* **2000**, *39*, 541.
[3] G. Merino, J. W. Jonker, E. Wagenaar, *Drug Metab. Dispos.* **2005**, *33*, 614.
[4] B. Narasimhan, D. Sharma, P. Kumar, *Med. Chem. Res.* **2012**, *21*, 26.
[5] K. Bielawski, S. Wołczyński, A. Bielawska, *Pol. J. Pharmacol. Pharm.* **2004**, *56*, 373.
[6] R. A. Haque, N. Hasanudin, M. A. Iqbal, A. Ahmad, S. Hashim, A. A. Majid, M. B. Khadeer Ahamed, *J. Coord. Chem.* **2013**, *66*, 3211.
[7] S. Bonham, L. O. Donovan, M. P. Carty, F. Aldabbagh, *Org. Biomol. Chem.* **2011**, *9*, 6700.
[8] F. Cachoux, T. Isarno, M. Wartmann, K. H. Altmann, *Chembiochem* **2006**, *7*, 54.
[9] X. Hou, F. Huang, J. M. Carboni, *Mol. Cell. Ther.* **2011**, *10*, 117.
[10] B. Narasimhan, D. Sharma, P. Kumar, *Med. Chem. Res.* **2011**, *20*, 1119.
[11] B. Narasimhan, D. Sharma, P. Kumar, *Med. Chem. Res.* **2012**, *21*, 269.
[12] F. Gümüş, Ö. Algül, G. Eren, H. Eroğlu, N. Diril, S. Gür, A. Özkul, *Eur. J. Med. Chem.* **2003**, *38*, 473.
[13] D. Kumar Sau, R. J. Butcher, S. Chaudhuri, N. Saha, *Mol. Cell. Biochem.* **2003**, *253*, 21.
[14] M. L. Teyssot, A. S. Jarrousse, M. Manin, *Dalton Trans.* **2009**, *35*, 6894.
[15] C. Graham, *Br. J. Nurs.* **2005**, *14*(Suppl. 5), S22.
[16] J. C. Garrison, W. J. Youngs, *Chem. Rev.* **2005**, *105*, 3978.
[17] A. Melaiye, R. S. Simons, A. Milsted, *J. Med. Chem.* **2004**, *47*, 973.
[18] L. Eloy, A. S. Jarrousse, M. L. Teyssot, A. Gautier, L. Morel, C. Jolivalt, S. Rolan, *ChemMedChem* **2012**, *7*, 805.
[19] B. Yığıt, Y. Gök, I. Özdemır, S. Günal, *J. Coord. Chem.* **2012**, *65*, 371.
[20] Y. Li, X. Dong, Y. Gou, Z. Jiang, H.-L. Zhu, *J. Coord. Chem.* **2011**, *64*, 1663.
[21] Y. Gök, S. Akkoç, O. Zelical, I. Özdemır, S. Günal, E. Sayin, *Turk. J. Chem.* **2003**, *37*, 1007.
[22] R. A. Haque, A. W. Salman, S. Budagumpi, A. A. Abdullah, A. M. Majid, *Metallomics* **2013**, *5*, 60.
[23] F. Almalioti, J. MacDougall, S. Hughes, M. M. Hasson, R. L. Jenkins, B. D. Ward, G. J. Tizzard, S. J. Coles, D. W. Williams, S. Bamford, I. A. Fallis, A. Dervisi, *Dalton Trans.* **2013**, *42*, 1237.
[24] R. A. Haque, M. A. Iqbal, P. Asekunowo, A. M. S. Abdul Majid, M. B. Khadeer Ahamed, M. I. Umar, S. S. Al-Rawi, F. R. S. Al-Suede, *Med. Chem. Res.* **2013**, *22*, 1663.
[25] M. A. Iqbal, R. A. Haque, S. Budagumpi, M. B. Khadeer Ahamed, A. M. S. Abdul Majid, *Inorg. Chem. Commun.* **2013**, *28*, 64.
[26] W. Liu, R. Gust, *Chem. Soc. Rev.* **2003**, *42*, 755.
[27] *ApexII*, Bruker AXS Ltd, Madison, WI, **2005**.
[28] G. M. Sheldrick, *Acta Crystallogr. A* **2008**, *64*, 112.
[29] L. J. Barbour, *J. Supramol. Chem.* **2001**, *1*, 189.
[30] W. L. Drew, A. L. Barry, R. O'Toole, J. C. Sherris, *Appl. Microbiol.* **1972**, *24*, 240.
[31] A. B. Lansdown, A. Williams, S. Chandler, S. Benfield, *J. Wound Care* **2005**, *14*, 155.
[32] I. Wiegand, K. Hilpert, E. W. R. Hancock, *Nat. Protoc.* **2008**, *3*, 163.
[33] N. Ramana, R. Jeyamurugan, A. Sakthivel, L. Mitu, *Spectrochim. Acta A* **2010**, *75*, 88.
[34] J. M. Hayes, M. Viciano, E. Peris, G. Ujaque, A. Lledós, *Organometallics* **2007**, *26*, 6170.
[35] S. Budagumpi, V. K. Revankar, *Transit. Met. Chem.* **2010**, *35*, 649.
[36] W. N. O. Wylie, A. J. Lough, R. H. Morris, *Organometallics* **2010**, *29*, 570.
[37] O. X. Liu, H. L. Li, X. J. Zhao, X. X. Ge, M. C. Shi, G. Shen, Y. Zang, X. G. Wang, *Inorg. Chim. Acta* **2011**, *376*, 437.
[38] S. Sakaguchi, M. Kawakami, J. O'Neill, K. S. Yoo, K. W. Jung, *J. Organometal. Chem.* **2010**, *695*, 195.
[39] I. Özdemir, H. Arslan, S. Demir, D. Van Derveer, B. Çetinkaya, *Inorg. Chem. Commun.* **2008**, *11*, 1462.
[40] P. C. B. Page, B. R. Buckley, S. D. R. Christie, M. Edgar, A. M. Poulton, M. R. J. Elsegood, V. McKee, *J. Organometal. Chem.* **2005**, *690*, 6210.
[41] R. A. Haque, M. A. Iqbal, S. Budagumpi, M. B. K. Ahamed, A. M. A. Majid, N. Hasanudin, *Appl. Organometal. Chem.* **2013**, *27*, 214.
[42] S. Demir, I. Özdemir, B. Cetinkaya, H. Arslan, D. Van Derveer, *Polyhedron* **2011**, *30*, 195.
[43] M. V. Baker, D. H. Brown, R. A. Haque, B. W. Skelton, A. H. White, *Dalton Trans.* **2004**, *21*, 3756.
[44] F. E. Hahn, *Angew. Chem. Int. Ed.* **2006**, *45*, 1348.
[45] M. Poyatos, J. A. Mata, E. Falomir, R. H. Crabtree, E. Peris, *Organometallics* **2003**, *22*, 1110.
[46] N. A. Piro, J. S. Owen, J. E. Bercaw, *Polyhedron* **2004**, *23*, 2797.

[47] W. Wang, F. Wang, M. Shi, *Organometallics* **2010**, *29*, 928.
[48] P. de Fremont, N. M. Scott, E. D. Stevens, T. Ramnial, O. C. Lightbody, C. L. B. Macdonald, J. A. C. Clyburne, C. D. Abernethy, S. P. Nolan, *Organometallics* **2005**, *24*, 6301.
[49] R. A. Haque, A. W. Salman, T. S. Guan, H. H. Abdallah, *J. Organometal. Chem.* **2011**, *696*, 3507.
[50] D. Pugh, J. A. Wright, S. Freeman, A. A. Danopoulos, *Dalton Trans.* **2006**, *6*, 775.
[51] A. Liu, X. Zhang, W. Chen, H. Qiu, *Inorg. Chem. Commun.* **2008**, *11*, 1128.
[52] Y. L. Murthy, G. Durga, A. Jha, *Med. Chem. Res.* **2013**, *22*, 2266.
[53] N. Ramana, R. Jeyamurugana, A. Sakthivel, L. Mitub, *Spectrochim. Acta A* **2010**, *7*, 88.
[54] I. Özdemir, E. O. Özcan, S. Günal, N. Gurbus, *Molecules* **2010**, *15*, 2499.
[55] A. R. Knapp, M. J. Panzner, A. D. Medvetz, B. D. Wright, C. A. Tessier, W. J. Youngs, *Inorg. Chim. Acta* **2010**, *364*, 125.
[56] R. Kumar, S. Obrai, A. Kaur, M. S. Hundal, H. Meehnian, A. K. Jana, *New J. Chem.* **2014**, *38*, 1186.
[57] I. Özdemir, N. Gürbüz, Ö. Doğan, S. Günal, İ. Özdemir, *Appl. Organometal. Chem.* **2010**, *24*, 758.
[58] R. A. Haque, P. O. Asekunowo, S. Budagumpi, *Inorg. Chem. Commun.* **2014**, *47*, 56.
[59] M. Viciano, E. Mas-Marza, M. Sanau, E. Peris, *Organometallics* **2006**, *25*, 3063.
[60] Q. L. Zhang, J. G. Liu, J. Z. Liu, H. Li, Y. Yang, H. Xu, H. Chao, L. N. Ji, *Inorg. Chim. Acta* **2002**, *339*, 34.
[61] R. A. Haque, P. O. Asekunowo, M. R. Razali, *Transit. Met. Chem.* **2014**, *39*, 281.
[62] N. Raman, T. Baskaran, A. Selva, *J. Iran Chem. Res.* **2008**, *1*, 29.

Supporting Information

Additional supporting information may be found in the online version of this article at the publisher's web-site.